International Journal of Greenhouse Gas Control 109 (2021) 103337

Contents lists available at ScienceDirect

International Journal of Greenhouse Gas Control

journal homepage: www.elsevier.com/locate/ijggc

Basalt powder as a supplementary cementitious material in cement paste for CCS wells: chemical and mechanical resistance of cement formulations for CO_2 geological storage sites

Gabriela Gonçalves Dias Ponzi [a,b], Victor Hugo Jacks Mendes dos Santos [a,b], Renan Bordulis Martel [a], Darlan Pontin [a], Amanda Sofia de Guimarães e Stepanha [a,b], Marta Kerber Schütz [a,c], Sonia C. Menezes [d], Sandra M.O. Einloft [a,b,c], Felipe Dalla Vecchia [a,b,c,*]

[a] Pontifical Catholic University of Rio Grande do Sul, PUCRS. Institute of Petroleum and Natural Resources, Avenida Ipiranga, 6681, – TECNOPUC, Building 96J, 90619-900, Porto Alegre, Brazil.
[b] Pontifical Catholic University of Rio Grande do Sul, PUCRS, Graduate Program in Materials Engineering and Technology, Avenida Ipiranga, 6681– Building 32, 90619-900, Porto Alegre, Brazil.
[c] Pontifical Catholic University of Rio Grande do Sul, PUCRS, School of Technology, Avenida Ipiranga, 6681 – Building 30, 90619-900, Porto Alegre, Brazil.
[d] Research and Development Center "Leopoldo Américo Miguez de Mello" (CENPES) - Petrobras; Avenida Horácio de Macedo, 950, 21941-915, Rio de Janeiro, Brazil.

ARTICLE INFO

Keywords:
Wellbore integrity
CO_2 storage
Cement degradation by CO_2
Basalt powder
Supplementary cementitious material

ABSTRACT

This study proposes the application of basalt powder (BP) as a supplementary cementitious material (SCM) in cement formulations for Carbon Capture and Storage (CCS) wells. From experimental results, we identified that the BP can be characterized as a filled-pozzolanic SCM, presenting low pozzolanic activity, large inert fraction, and particle size significantly smaller than class G cement. Formulations with low basalt powder ($\leq$ 0.5 wt.%) content presented the greatest potential for application in CCS wells since they are more resistant to CO_2 degradation, showing low porosity and suitable mechanical properties, as evidenced in carbonation tests. Due to basalt powder characteristics, we conclude that the increase in the chemical resistance of the cement formulation with low BP content is due to the reduction of both the porosity and permeability as a result of filling of empty spaces and the refinement of the porous cement network, allied to the low reduction of the alkaline reserve of portlandite. The combination of these features increases the material's resistance to fluid intrusion, reduces the progress of the CO_2 degradation front, and preserves the cement matrix's ability to delay the reaction of acid gases.

1. Introduction

Constant economic growth and high consumption of natural resources continue to increase the demand for energy, especially that derived from fossil fuels (Bai et al., 2016). The intense use of energy resources derived from coal and oil results in considerable CO_2 emissions into the atmosphere contributing significantly to global warming (Metz et al., 2005). Carbon Capture and Storage (CCS) was proposed as a transition technology to decarbonize the economy, reducing the human ecological footprint and partially mitigating climate change (Bai et al., 2016; Ketzer et al., 2009; Koukouzas et al., 2017; Tiong et al., 2019). From this approach, it is expected that after being widely implemented, CCS can store approximately 5 billion tons of CO_2 per year (Tiong et al., 2019).

CCS technologies have been studied from conceptual assessments to implementation in large-scale projects, as a technology to permanently store CO_2 in geological formations such as coal seams, depleted oil and gas fields and deep saline aquifers (Abid et al., 2018; Iglesias et al., 2015; Metz et al., 2005; Tiong et al., 2019). In this process, an essential step to access the deep geological formations is carrying out drilling and well completion (Carroll et al., 2016; Torsæter et al., 2015; Wakeel et al., 2019). In wellbore construction, cementation is a key step of successful CCS operations. The cement sheath protects the steel casing, stabilizes the geological formation and generates the hydraulic seal that prevents the uncontrolled flow of fluids in the storage site through a tight bond between the formation-cement-casing system (Jobard et al., 2018;

* Corresponding author.
E-mail addresses: victor.santos@pucrs.br (V.H.J.M. Santos), marta.schutz@pucrs.br (M.K. Schütz), felipe.vecchia@pucrs.br (F.D. Vecchia).

https://doi.org/10.1016/j.ijggc.2021.103337
Received 3 September 2020; Received in revised form 30 March 2021; Accepted 12 April 2021
Available online 9 May 2021

Tremosa et al., 2017). However, the same structures used for CO_2 injection into the reservoirs can constitute potential paths for gas leakage into shallow geological structures, or back to the atmosphere (Abid et al., 2018; Carroll et al., 2016; Dong et al., 2020). Thus, ensuring the wellbore integrity throughout its life cycle (construction, injection, monitoring and abandonment) is a key issue for CCS projects (Kiran et al., 2017; Omosebi et al., 2017; Postma et al., 2019).

In CCS storage sites, the presence of acid gases, such as supercritical CO_2, creates additional problems related to cement degradation and steel casing corrosion (Kiran et al., 2017; Postma et al., 2019; Torsæter et al., 2015; Wakeel et al., 2019). Thus, it is necessary to ensure that all materials used in the wellbore construction are able to withstand geological conditions for long periods, ensuring the quality of the hydraulic seal and preventing uncontrolled fluids circulation along the reservoir (Dong et al., 2020; Omosebi et al., 2017). Among materials used in the wellbore construction, cement has been receiving special attention from the academic community and Oil & Gas companies, since its components are not stable in CO_2-rich environments (Teodoriu and Bello, 2020; Wang et al., 2017). From laboratory scale studies to field sampling, it is widely documented that cement is susceptible to significant changes when exposed to supercritical CO_2, so compromising the wellbore integrity and the permanent carbon storage (Abid et al., 2020, 2018; Carey et al., 2007; Szabó-Krausz et al., 2020; Teodoriu and Bello, 2020).

API cement formulations (A-H) meet poor specific CCS design requirements and show no adequate chemical stability in CO_2-rich environments. Thus, Oil & Gas companies are constantly searching for an adequate solution to increase well integrity in CO_2-rich environments (Tiong et al., 2019). The use of supplementary cementitious materials (SCM) (Abid et al., 2020; Ledesma et al., 2020; Schütz et al., 2019; Sedić et al., 2020), nanomaterials (Abid et al., 2020; Mahmoud and Elkatatny, 2019; Tiong et al., 2019), polymers (Baldissera et al., 2017b, 2017a; Schütz et al., 2019) and composites (SCM reinforced polymers) (Schütz et al., 2019, 2018) has been highlighted as possible alternative to improve cement chemical resistance. However, it is required further studies to evaluate the performance of these materials in representative conditions of CCS storage sites.

Thus, once the drilling of the well progresses to deeper reservoirs, with more adverse pressure and temperature conditions, it is necessary to develop new cement formulations that can meet design requirements and are able to resist a long-term exposure to CO_2 (Iyer et al., 2018; Omosebi et al., 2016; Postma et al., 2019; Wang et al., 2017). Among the most common strategies for changing cement properties is the use of SCM in paste formulations, which alter the composition of the cement minerals, its porous structure, and the material's chemical and mechanical resistance (Abid et al., 2020; Ghafari et al., 2016; Ledesma et al., 2020; Lothenbach et al., 2011; Paris et al., 2016; Tiong et al., 2019; Yin et al., 2018). These novel formulations must be studied under appropriate conditions, similar to those found in the CCS storage site, in order to assess the extent of the CO_2 degradation process and guarantee the wellbore integrity throughout its life cycle, thereby avoiding or delaying the need for workover operations (Abid et al., 2020; Costa et al., 2019; Dong et al., 2020; Szabó-Krausz et al., 2020; Teodoriu and Bello, 2020).

So far, there is no definitive solution to increase well integrity in CO_2-rich environments. Research on evaluating the chemical and mechanical properties of cement formulations modified by SCM against degradation due to CO_2 is limited, and only a few SCMs have been evaluated (Abid et al., 2020; Ledesma et al., 2020; Yin et al., 2018). However, it is recognized that even a small amount of SCM can result in a change in the amount and type of hydration products formed in the cement matrix, and can promote a refinement of the porous structure, which could delay the carbonation process and improve the wellbore integrity (Ghafari et al., 2016; Lothenbach et al., 2011; Paris et al., 2016; Yin et al., 2018). Furthermore, there is no consensus solution on the use of SCM (conventional or unconventional) in cement formulations to reduce the effect of acid gases (Tiong et al., 2019). Thus, there are many issues to be addressed about the type and quantity of SCM that must be added to adjust the properties of the cement paste for application in CO_2-rich environment. Therefore, an adequate understanding of the cement carbonation process can allow to obtain properties of the new formulations to be adjusted to the requirements of the future CCS projects (Teodoriu and Bello, 2020).

In this context, basalt powder (BP), a natural SCM, could be added to cement formulations in order to improve the material's resistance against long-term exposure to CO_2 (Abid et al., 2020; Dobiszewska and Beycioğlu, 2017; El-Didamony et al., 2015; Laibao et al., 2013; Saraya, 2014; Shapakidze et al., 2017; Zhang et al., 2018). Basalt is described as igneous rock that can be used as an SCM with low pozzolanic activity, as a replacement for the cement powder or as an additive to the cement paste in new cement formulations (El-Didamony et al., 2015; Hassaan, 2001; Laibao et al., 2013; Saraya, 2014). Basalt powder is a by-product from the mining process and its use in cement paste for wells can represent an environmental and financial gain, since the cost of the raw material is lower and part of the CO_2 emission, from clinker processing, is avoided (Dobiszewska and Beycioğlu, 2017; Laibao et al., 2013; Shapakidze et al., 2017; Zhang et al., 2018). Basalt powder is readily available and has characteristics that recommend its use as an SCM, so making it a potential candidate to serve as an SCM on a commercial scale.

Previously, Jadid and Okandan (2011) evaluated the chemical resistance of cement paste formulations with the addition of basalt at a concentration of 0%, 6%, 9% and 13%. Despite obtaining positive results, the work based its conclusions on only four cement specimens (one per formulation), which underwent a degradation process in brine solution under mild experimental conditions (65°C and 75.8 bar CO_2). Furthermore, a complete characterization of the cement formulations after exposure to CO_2 was not performed, due to the compromise of some specimens after the degradation test. Thus, the present work proposes the first comprehensive study on the use of basalt powder as SCM in well cement formulations to improve the material performance in supercritical CO_2-environment. The BP was added in different concentrations to the API class G cement, and the cement paste carbonation was carried out simulating CCS reservoir conditions. The new formulations were studied to evaluate the effect of the adding basalt powder on the properties of the cement paste, to define the ideal mixture composition, and indicating which one presents the best chemical/mechanical performance. The evaluation of the chemical and mechanical performance of new materials when exposed to supercritical CO_2 was carried out by a comprehensive experimental characterization. Thus, from the addition of natural SCM, we aim to propose new cement formulations capable of increasing the wellbore integrity in CCS operations and present a low-cost solution to improve cement paste stability in CO_2-rich environment.

2. Materials and Methods

The present work evaluates the integrity of cement paste formulations prepared from the mixture of API class G cement and BP as an SCM. The new formulations, prepared from the addition of BP contents at 0.25 to 5% by weight, were subjected to wet carbonation under CO_2 supercritical conditions, simulating the CCS storage environment. Formulations were evaluated by a series of analytical methods before and after undergoing the CO_2 degradation process.

2.1. Materials

The chemicals: calcium oxide (Êxodo, 95%), hydrochloric acid (Química Moderna, 37%), saccharose (Synth, analytical grade) and phenolphthalein (Química Moderna, analytical grade) were used without further purification. The cement used in this study was an API class G cement (Lafarge Holcim), the composition of which is shown in

Table 1
Class G Portland cement chemical composition and specific surface area.

Chemical composition	Percentage [%]
SiO_2	29.25
Al_2O_3	3.95
Fe_2O_3	4.57
CaO	65.07
MgO	2.32
SO_3	2.27
Na_2O	0.25
K_2O	0.33
Class G Characterization	**Surface area [$m^2 \cdot g^{-1}$]**
BET specific surface area	0.77
Langmuir specific surface area	2.69
[a]Average particle size (Å)	78,103.0

[a] Estimated based on the specific surface area analysis.

Table 1.

Basalt was donated from local suppliers in the form of a coarse aggregate for civil construction, and the BP was obtained through ball milling and material sieving. Thus, BP was obtained by grinding 500 grams of coarse aggregate in the De Leo 0907 ball mill, for 60 hours, with a rotation of 150 rpm in an external 17.8 × 17.8 cm cylinder. The load of grinding steel balls was: Ø50 mm balls (5 units), Ø40 mm balls (5 units), Ø32 mm balls (5 units), Ø15 mm balls (5 units), Ø25 mm balls (24 units), Ø19 mm balls (15 units) and Ø10 mm balls (21 units). After grinding, the powder was sieved manually from mesh #200, followed by #230, #270 and #325 mesh sieve. Thus, only the powder passed through the #325 mesh sieve were used in this work as SCM. Furthermore, the financial assessment of the basalt powder addition to wellbore cement formulations was carried out and the results will be presented later.

2.2. Sample preparation

All formulations were prepared following the recommendations of API 10A and 10B standards (API Specification, 2010, 2000). The mixing water was calculated based only on the dry cement fraction (water-cement ratio of 0.44) and the BP content was not compensated. Thus, prepared well cement formulations have a water-to-solids ratio (W/S) ranging from 0.440 (class G neat cement) to 0.419 (5% basalt powder formulation). To prepare the cement paste, dry blending of cement and BP was previously performed, and the mixtures were prepared by adding water in a Chandler Engineering mixer (Model 3260) for 15 s at 4,000 rpm and 35 s at 12,000 rpm. Then, the cement pastes were poured into PVC molds, as shown in the Supplementary Material (Figure S1), followed by curing in a thermostatic bath (65°C and atmospheric pressure) for 14 days. After the wet thermostatic cure, the cement specimens were cut, using a low-speed cutter (Isomet), to the dimensions of 22 mm in diameter x 44 mm in height. Thus, a portion of the specimens (non-carbonated samples) were reserved in a calcium hydroxide solution, while the other specimens (carbonated samples) were used for the CO_2 degradation experiments.

2.3. CO_2 degradation experiments

CO_2 degradation experiments were conducted in a HPHT (high pressure-high temperature) pressure vessel, as shown in Figure S2 (Supplementary Material). Cement specimens were exposed to a supercritical CO_2-deionized water system at 65°C, 15 MPa for 7 days. The applied quasi-static environment is reported as the most appropriate model to simulate the well dynamics in a CCS storage site (Bagheri et al., 2018; Teodoriu and Bello, 2020), since no continuous fluid channels seem to be widespread in these geological formations (Lavrov, 2018). At the end of the experiments, chemical and physical evaluations were performed, the results being compared to the respective non-carbonated samples.

2.3.1. Cement paste carbonation reactions

CO_2 dissolution in water results in the production of $H_2CO_{3\,(l)}$, $HCO_{3\,(l)}^-$ and/or $CO_{3\,(l)}^{2-}$, depending on the medium pH (Bai et al., 2015; Duguid et al., 2011; Kiran et al., 2017). These reactions are represented by Equation 1.

$$CO_{2(g)} + H_2O_{(l)} \leftrightarrow H_2CO_{3(l)} \leftrightarrow HCO_{3\,(l)}^- + H^+_{(l)} \leftrightarrow CO_{3\,(l)}^{2-} + 2H^+_{(l)} \quad (1)$$

Cement is a complex matrix, composed of a series of hydrated products, which can react with carbon species in aqueous solution (H_2CO_3, HCO_3^- and /or CO_3^{2-}) (Lorek et al., 2016). According to the literature, the main reactions result in the consumption of $Ca(OH)_2$ or portlandite (CH) and calcium silicate hydrate (C-S-H) phases to produce different calcium carbonate ($CaCO_3$) polymorphs, such as calcite, aragonite and vaterite (Duguid et al., 2011; Koukouzas et al., 2017; Tiong et al., 2019). These reactions are represented by Equations 2-7.

$$Ca(OH)_{2(s)} + CO_{3\,(l)}^{2-} + 2H^+_{(l)} \rightarrow CaCO_{3(s)} + 2H_2O_{(l)} \quad (2)$$

$$Ca(OH)_{2(s)} + HCO_{3\,(l)}^- + H^+_{(l)} \rightarrow CaCO_{3(s)} + 2H_2O_{(l)} \quad (3)$$

$$C-S-H_{(s)} + CO_{3\,(l)}^{2-} + 2H^+_{(l)} \rightarrow CaCO_{3(s)} + SiO_xOH_{x(s)} \quad (4)$$

$$C-S-H_{(s)} + HCO_{3\,(l)}^- + H^+_{(l)} \rightarrow CaCO_{3(s)} + SiO_xOH_{x(s)} \quad (5)$$

$$CaCO_{3\,(s)} + CO_{2\,(g)} + H_2O_{(l)} \leftrightarrow Ca^{2+} + HCO_{3\,(l)}^- \quad (6)$$

$$CaCO_{3\,(s)} + 2H^+_{(l)} \leftrightarrow CO_{2\,(g)} + H_2O_{(l)} + Ca^{2+} \quad (7)$$

2.4. Sample characterization

In the present work, pozzolanic activity analysis (modified Chapelle test), surface area analysis (Brunauer–Emmett–Teller and Langmuir), mineral composition estimation by X-ray diffraction (XRD) analysis, and microscopy analysis by scanning electron microscopy with energy dispersive spectroscopy (SEM-EDS) were applied to characterize the basalt powder, while SEM-EDS, carbonation test (phenolphthalein cement indicator), carbonated layer analysis, compressive strength analysis, and X-ray microtomography analysis (MicroCT) were carried out to analyze the non-carbonated and carbonated cement specimens.

2.4.1. Pozzolanic activity analysis

To assess the basalt powder pozzolanic activity, the modified Chapelle method was applied following the recommendations of the Brazilian standard (NBR 15895) (ABNT, 2010). The SCM pozzolanic activity is estimated from the calcium hydroxide content fixed by the Chapelle method, expressed in milligrams (mg) of $Ca(OH)_2$ consumed per gram (g) of mineral. As defined by Raverdy et al. (1980), 330 mg $Ca(OH)_2$ is a threshold value for an SCM to be considered as a pozzolanic material with high activity.

2.4.2. Specific surface area analysis

The analysis of cement and basalt powder specific surface areas by BET (Brunauer, Emmett and Teller) and Langmuir isotherms were performed in the TriStar II Plus surface area and porosity analyzer. The samples were previously submitted to a high vacuum degassing system for 3 h to 24 h and the adsorption analysis was carried out using liquid N_2 (-195.85°C).

2.4.3. X-ray diffraction analysis

X-ray diffraction analysis was carried out using a diffractometer from Shimadzu (XRD 700) at voltage of 40 kV, current of 30 mA with Cu-Kα radiation and a scanning step size 0.02° in the θ-2θ ranging from 2 to

80°.

2.4.4. Microscopy analysis

Microscopy analysis by SEM-EDS was performed in the Inspect F50 - FEI microscope to: (A) characterize the morphological structure of BP and evaluate the chemical composition of some microconstituents, (B) characterize the structure of the cement paste, (C) evaluate the extent of the degraded layer in the cement specimens after the reaction with supercritical CO_2 and (D) analyze the elemental profile of the cement specimens after the carbonation process (linear and mapping EDS scanning).

2.4.5. Carbonation test

For the carbonated layer analysis, specimens were cut longitudinally with a low-speed cutter and diamond cutting disc. Then, phenolphthalein in ethyl alcohol-water solution (2%) (48:50 v%) was sprayed on the samples to assess the extent of the cement carbonation reaction. The carbonation test used is based on the interaction of the phenolphthalein solution with the cement alkaline reserve (portlandite). Thus, the indicator highlights the boundary between the non-carbonated area of the cement specimens (pink fraction) and the degraded layer (non-pigmented carbonated fraction).

2.4.6. Carbonated layer analysis

The estimation of cement carbonated layer thicknesses was carried out by using image processing software based on the phenolphthalein sprayed images. For each formulation, three cement specimens with several measurements were used to obtain the average carbonated layer thickness.

2.4.7. Compressive strength analysis

Compressive strength analysis was performed on the cement specimens using a Universal Testing Machine (UTM) from Shimadzu (300 kN). The compression tests parameters, such as speed of analysis, dimensions of the cement specimens and number of replications, meet the specifications described by the ASTM C39 standard (ASTM International, 2018).

2.4.8. X-ray microtomography analysis (MicroCT)

X-ray microtomography analyses were performed on the cement specimens using the Skyscan 1173 X-Ray Microtomograph (Bruker) following the manufacturer's recommendations. From the MicroCT data, the carbonated volume and porosity were estimated.

2.5. Data analysis

Univariate statistical methods are sometimes inefficient to evaluate the data derived from complex systems such as the cement carbonation under a reservoir environment. Thus, the data analysis of the present work was carried out by the Principal Component Analysis (PCA), Hierarchical Clustering Analysis (HCA) and Correlation Analysis (CA) using the Solo+MIA software (Eigenvector Research). PCA and HCA are exploratory analysis tools applied to represent large datasets in a small dimensional space, while the CA performs the evaluation of the linear relationship between all the evaluated parameters. From this approach, it is possible to evaluate the cause/effect relationship of adding BP into well cement formulations. Since the parameters are measured in different units, it is necessary to autoscale and mean center the data before the PCA analysis to ensure that all variables have the same weight in the multivariate analysis.

3. Results and Discussion

3.1. Basalt powder characterization

Basalt powder was used as an SCM in well cement formulations, being initially characterized by means of SEM and specific surface area analyses to evaluate the morphological, rheological, and physical effects in the cement–BP formulations. The basalt powder SEM image is shown in Fig. 1, while the specific surface area results are shown in Table 2.

Basalt powder (Fig. 1) presented different particle sizes with irregular shape, rough surface and varied granulometry. While the larger particles show undefined rounded edges, which may be related to the basic fragmentation mechanism of abrasion after the ball milling process (Moosakazemi et al., 2017), the smaller particles show irregular shapes, rough surface and sharper edges, which may be associated with the different cleavage planes due to the diversified mineralogical composition of the basalt (Laibao et al., 2013).

When comparing the BET specific surface area of basalt powder (5.41 $m^2 \cdot g^{-1}$ - Table 2) with class G cement (0.77 $m^2 \cdot g^{-1}$ - Table 1) we observe that the BP has higher specific surface area and smaller particle size. Thus, it is expected that the BP particle morphological and surface characteristics are relevant to the mechanical and rheological properties of the cement paste (Laibao et al., 2013; Liu et al., 2018; Ouyang et al., 2018). While the irregular shapes of the smaller particles confer a high relative specific surface area, contributing to the decrease of the cement paste hydration and to the reduction of pore size and permeability of the cured material (Liu et al., 2018), the slightly rounded edges of the bigger particles improve the flowability of the cement paste and reduce the material stress concentration, making the specimens harder to crack (Laibao et al., 2013; Ouyang et al., 2018). Furthermore, particles with sharper edges usually create more resistance to the mixture rheology and increase the water demand for cement hydration due to increased specific surface area (Laibao et al., 2013). The small BP content added to the proposed cement formulation resulted in a slight difference from the cement without BP addition.

After identifying the morphological and surface characteristics of the basalt powder, the mineral composition of the raw material was characterized by means of XRD (Table 2 and Figure S3). The mineral composition of SCM defines its reactivity during the hydration process, the role performed by the additive in the cement formulation, and indicates which are the mineral phases that will be generated after the curing process (Lothenbach et al., 2011; Paris et al., 2016; Yin et al., 2018).

From the XRD pattern results (Table 2), it was identified that BP is mostly composed of Andesine (37.8%), Augite (27.9%), Orthoclase (11.4%) and Quartz (9.9%), while it also presented minority mineral phases composed of Sanidine (5.4%), Magnetite (3.1%), Ilmenite (2.5%), Forsterite iron (1.6%) and Goethite (0.3%). All identified minerals have been previously reported in basalt powders applied as SCM in cement and concrete formulations (Hassaan, 2001; Labbaci et al., 2017; Laibao et al., 2013; Saraya, 2014), and indicate that BP may have a slightly pozzolanic activity throughout the hydration process so consuming cement portlandite and increasing the production of C-S-H phases (Laibao et al., 2013; Saraya, 2014), and/or presenting a filler effect due to the smaller particle size, reducing the cement porosity when occupying the empty spaces of the cured material (El-Didamony et al., 2015; Zhang et al., 2018).

To complement the morphological, mineralogical, and surface area analyzes, the pozzolanic activity (Table 2) of the basalt powder was evaluated using Chapelle's method. Chapelle's analysis assesses the pozzolanic activity of SCM based on the indirect measurement of portlandite consumption throughout the hydration process, so it is possible to verify the role that BP will play in the cement paste formulation. The higher the consumption of portlandite, the greater the formation of secondary mineral phases in the cementitious matrix (Ismail et al., 2020; Lothenbach et al., 2011). These reactions influence the chemical and physical properties of the cement paste, reducing porosity, increasing compressive strength and reducing chemical degradation by CO_2 (Ismail et al., 2020; Ledesma et al., 2020).

Based on the pozzolanic activity, BP consumed 180.2 mg $Ca(OH)_2$ during the Chapelle test, which is less than the 330 mg $Ca(OH)_2$ that is

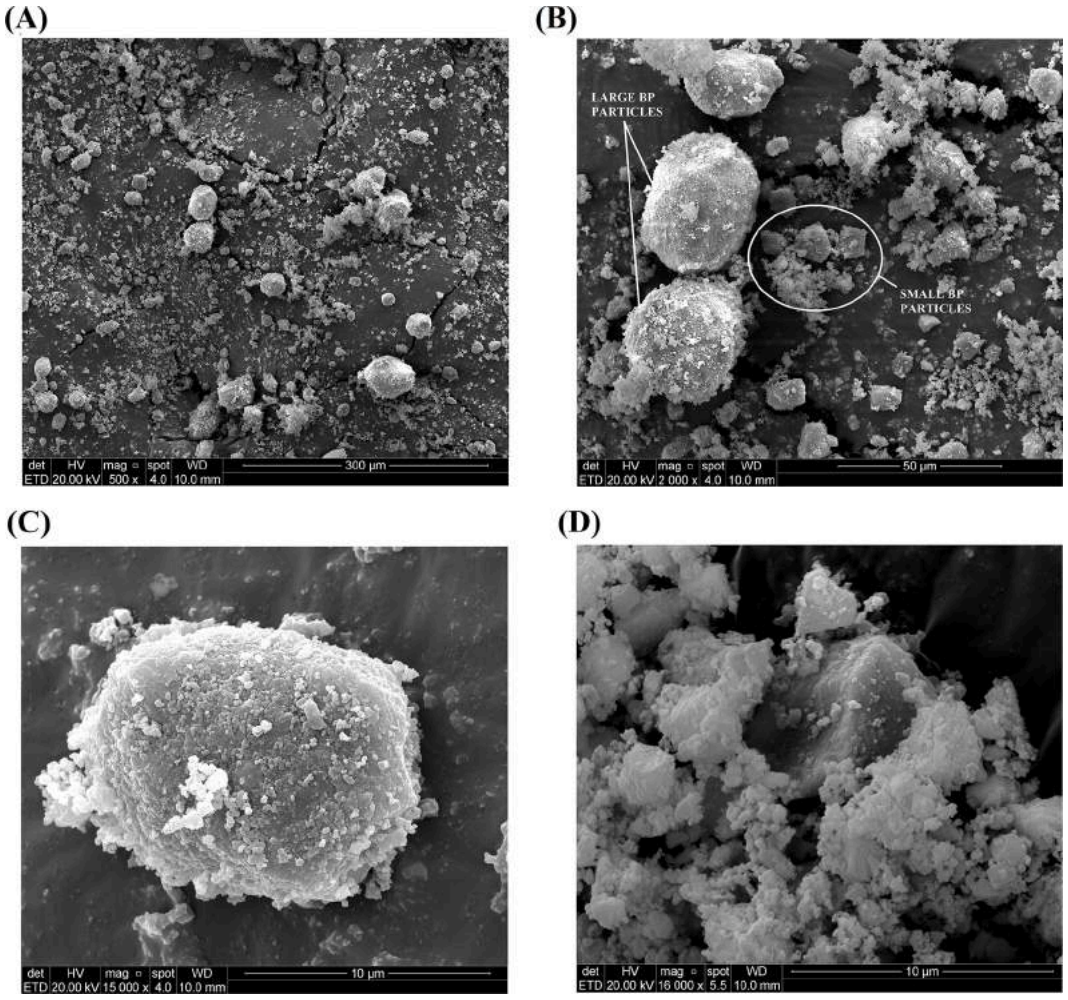

Fig. 1. SEM image showing different shapes of basalt powder with magnification of (A) 500x, (B) 2000x with large and small BP particles indicated, (C) 15000x of larger BP particle and (D) 16000x of small BP particle.

Table 2
Mineral composition, specific surface area and pozzolanic activity of basalt powder.

XRD Mineral Composition	Abbreviation	Value
Quartz [wt.%]	Q	9.9
Andesine [wt.%]	A	37.8
Sanidine [wt.%]	S	5.4
Augite [wt.%]	Px	27.9
Forsterite iron [wt.%]	F	1.6
Ilmenite [wt.%]	I	2.5
Goethite [wt.%]	G	0.3
Orthoclase [wt.%]	O	11.4
Magnetite [wt.%]	M	3.1
Basalt Powder Characterization	**Abbreviation**	**Value**
BET specific surface area [$m^2 \cdot g^{-1}$]	BET	5.41
Langmuir specific surface area [$m^2 \cdot g^{-1}$]	LSA	51.22
Pozzolanic Activity Index [mg $Ca(OH)_2$]	$I_{Ca(OH)2}$	180.2
[a] Average particle size (Å)	APS	11,097.3

[a] Estimated based on the specific surface area analysis.

defined by Raverdy et al. (1980) as a threshold value for a SCM to be considered as a pozzolanic material with high activity. Although BP has a large amount of minerals rich in silica and alumina, the low pozzolanic activity has been previously identified (El-Didamony et al., 2015; Laibao et al., 2013; Saraya, 2014), and is explained due to the lack of vitreous phases and the presence of high crystallized minerals (Benezet and Benhassaine, 1999; Snellings et al., 2012). Thus, based on the characterization results (Table 2), basalt powder can be used as filled-pozzolanic material, being partially consumed in the cement hydration process, and occupying the porous spaces of the material.

It is known that curing conditions (temperature and pressure) can influence the properties of the cement sheath. To prevent strength retrogression in wells operating at temperatures above 110°C, 35% to 40% of crystalline silica is added in relation to the weight of the cement (BWOC) (Bjørge et al., 2019). Unlike crystalline silica, an additive with high pozzolanic activity (Kuzielová et al., 2018), BP has low reactivity and large inert mineral fraction. Thus, due to low pozzolanic activity of the basalt powder, it is unlikely that BP can be used to replace crystalline silica as an additive in high-temperature well cement formulations. Therefore, future work should evaluate the feasibility of using mixtures of crystalline silica and basalt powder in high-temperature CCS wellbores cement, as well as studying the effect of CO_2 on the chemical and mechanical resistance of these formulations.

3.2. Chemical resistance of cement formulations

After characterizing the basalt powder and preparing the cement formulations, the CO_2 degradation tests were performed to evaluate the chemical resistance of the cement specimens. Fig. 2 shows images obtained from the BP 0.00 (neat cement paste) and BP 0.25 (cement paste containing BP 0.25 wt.%) samples after exposure to CO_2-saturated water at 15 MPa and 65°C for 7 days, illustrating the chemically altered layer

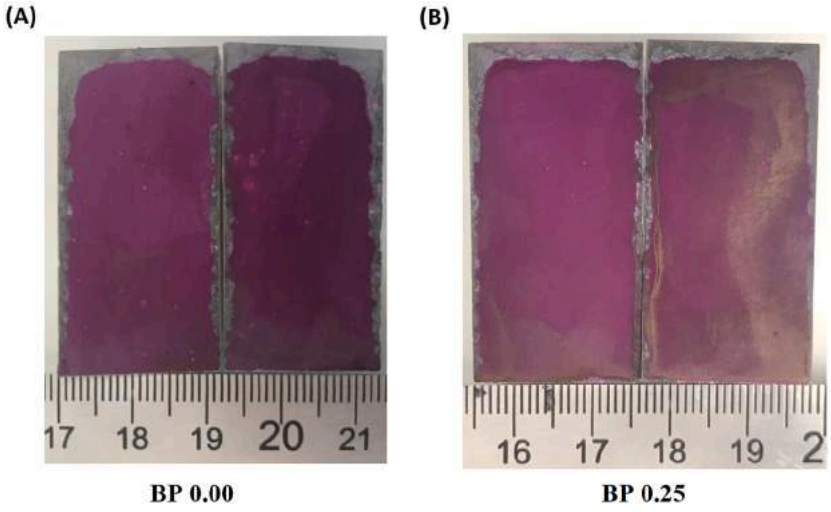

Fig. 2. Carbonated layer obtained after 7 days exposure to CO_2-water environment at 65 °C and 15 MPa: (A) BP 0.00 and (B) BP 0.25.

depth which is highlighted using phenolphthalein solution.

From the carbonation results, typical behavior of CO_2 degradation to the cement matrix was noticed from the reduction of the pink area and an increase of the carbonated grey area, highlighting the degraded fraction of the material (Ashraf, 2016; Costa et al., 2019; de Sena Costa et al., 2018; Qin and Gao, 2019; Zha et al., 2019). The pink color, observed in the central portion of the cement specimens, is associated with the interaction of the phenolphthalein solution with the alkaline reserve of the cement paste, which is mainly due to the preservation of the portlandite (CH) fraction indicating an absence of the CO_2 degradation process. Otherwise, the grey portion at the edges of the cement specimens demonstrates that there is high consumption of CH, indicating the neutralization of pH and the formation of calcium carbonates ($CaCO_3$) (Ashraf, 2016; Costa et al., 2019; de Sena Costa et al., 2018; Qin and Gao, 2019; Zha et al., 2019).

The reference cement paste (BP 0.00 - Fig. 2A) shows an extended degraded layer in comparison with BP 0.25 (Fig. 2B). These results suggest that the addition of the mineral filler improved the cement chemical performance when exposed to the corrosive medium with supercritical CO_2. Moreover, it can be assumed that the addition of basalt powder reduced the permeability of the sample, making the cement paste more resistant to CO_2 intrusion.

The chemical resistance of the cement formulations was evaluated by measuring the carbonated layer (CL) and carbonated volume (CV) of the specimens. Results are shown in Table 3. Since the degradation fronts do not advance homogeneously along the specimen, the CV was also estimated to obtain a more accurate measurement of the degraded fraction of the cement specimens.

Table 3 shows that, from the addition of BP in the cement, there is an initial reduction of the carbonated layer in relation to the reference (BP 0.00) and the best result was obtained for the formulation containing 0.25 wt.% of basalt powder (BP 0.25). Then, the extent of the carbonated volume increases from the BP 0.50 to BP 5.00, demonstrating that small additions of SCM are able to increase the material resistance against CO_2 chemical degradation, while higher basalt powder contents reduce the chemical resistance of the cement formulations. Furthermore, cement formulations with higher water-to-solids ratio, BP 0.25 (W/S = 0.439) and BP 0.50 (W/S = 0.438), have greater resistance to carbonation than samples with higher density: BP 1.00 (W/S = 0.436), BP 2.50 (W/S = 0.429) and BP 5.00 (W/S = 0.419). From these results, we found that cement formulations with low basalt powder content ($\leq$ 0.50 wt.%) shows the best chemical resistance to CO_2, confirming the literature statement that even small SCM additions can significantly alter the properties of the cement paste (Ghafari et al., 2016; Lothenbach et al., 2011; Paris et al., 2016; Yin et al., 2018). However, the literature argues that cement formulations with higher density are expected to have greater resistance to carbonation (Costa et al., 2019; Torsaeter et al., 2013). This change may be related to the basalt powder characteristics and will be addressed throughout the work.

Table 3
Chemically altered layer of cement specimens caused by the CO_2 degradation process during 7 days under 15 MPa and 65°C.

Sample	BP [wt.%]	W/S	CL[a] [mm]	CV[b] [mm^3 %]
BP 0.00	0.00	0.440	1.25 ± 0.58	20.40
BP 0.25	0.25	0.439	0.86 ± 0.11	15.91
BP 0.50	0.50	0.438	1.17 ± 0.17	19.73
BP 1.00	1.00	0.436	1.21 ± 0.23	20.65
BP 2.50	2.50	0.429	1.21 ± 0.18	32.83
BP 5.00	5.00	0.419	1.06 ± 0.05	30.15

BP - Basalt Powder; W/S – Water-to-Solids Ratio; CL - Carbonated Layer; CV - Carbonated Volume.
[a] estimated by the phenolphthalein test.
[b] estimated by MicroCT analysis.

3.2.1. *Cement paste microstructure analysis*

After evaluating the extent of the carbonation process in cement formulations, the samples were analyzed by SEM-EDS to assess the influence of the BP addition on the microstructure of the cement paste. Thus, from a longitudinal section, an SEM-EDS linear scan analysis was carried out (Fig. 3).

The cement paste degradation process by carbonic acid is characterized by different chemical reactions and multiple degradation zones with unique characteristics, due to several reactions that establish chemical equilibrium, through the dissolution and precipitation of different mineral phases Duguid et al., 2011; Koukouzas et al., 2017; Rochelle et al., 2004; Tiong et al., 2019). As soon as CO_2 turns into carbonic acid (Equation 1) and flows into the cement matrix, the first response of the cement paste to the pH change is the leaching of the calcium and hydroxyl ions from portlandite into the pores' water, forming a dissolution zone (Bai et al., 2015; Duguid et al., 2011; Rochelle et al., 2004). This region can be easily discerned in the SEM image of the BP 0.00 (Fig. 3A) and BP 0.25 (Fig. 3B) specimens by the presence of a highly porous area between unaltered cement paste and a high-density carbonated zone, characterized by the formation of calcium carbonate ($CaCO_3$) within the cement pores (Equations 2-(5), acting as an expansive pore blocking agent (Borges et al., 2010).

Initially, the calcium carbonate formation is considered beneficial, reducing the degradation kinetics, increasing the cement compressive

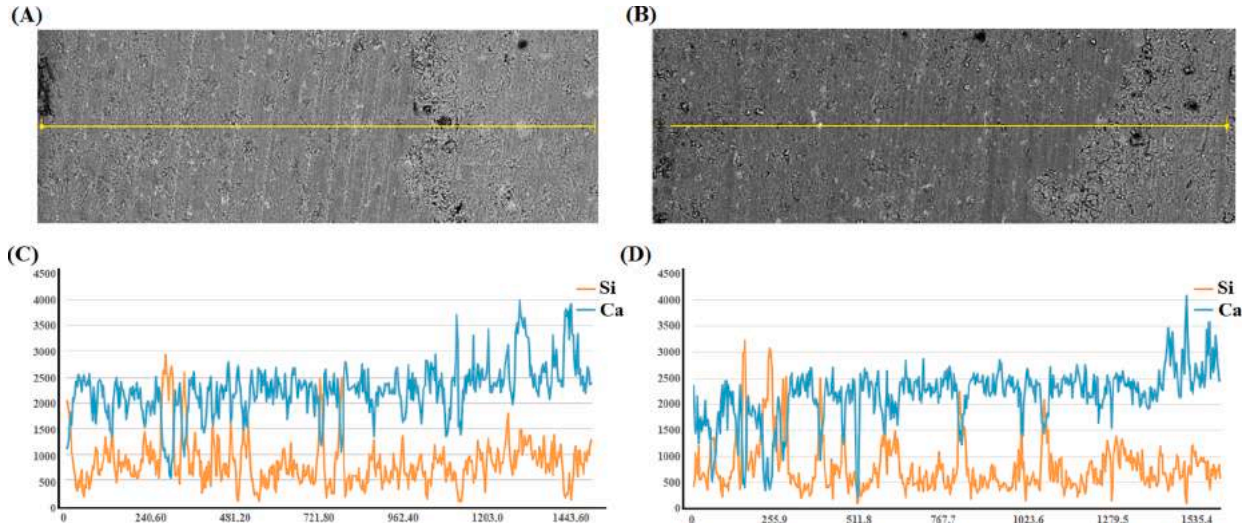

Fig. 3. SEM-EDS analysis of carbonated cement specimens: (A) BP 0.00, (B) BP 0.25, (C) EDS linear scan analysis of BP 0.00 and (D) EDS linear scan analysis of BP 0.25.

strength, decreasing the porosity and delaying the CO_2 diffusion (Borges et al., 2010). However, as the degradation process evolves, the portlandite reserve is depleted and pH of the pore solution is reduced so showing an acid characteristic. Then, at this degradation stage, the calcium carbonate can be transformed into highly leachable calcium bicarbonates (Equation 6), increasing the porosity and leading to an increase in the material pore pressure (Kutchko et al., 2008, 2007). In addition to $CaCO_3$ dissolution (Equation 7), the reduced pH allows the degradation of cement anhydrous phases, such as C_2S and C_3S, and of calcium silicate hydrate (C-S-H) by CO_2-rich fluids (Bertos et al., 2004; Kutchko et al., 2007; Mosleh et al., 2017). Then, after consuming the alkaline reserve of the cement, the C-S-H transformation process into calcium carbonate and amorphous silica occurs by leaching Ca^{2+} from the C-S-H structure, so decreasing the Ca/Si ratio and increasing the porosity of the cement paste. Although the degradation of C-S-H cannot be clearly seen in Fig. 3A and Fig. 3B, a downward trend in the Ca/Si ratio can be observed in Fig. 3C and Fig. 3D. Thus, the formation of calcium-rich (with a high content of calcium carbonate) and silicon-rich (with a high concentration of amorphous silica) phases can be clearly seen through SEM-EDS elementary mapping (Fig. 4).

From Fig. 4, the formation of different phases throughout the degradation process may be seen in the carbonated layers. Both BP 0.00 and BP 0.25 cement specimens show degradation zones with signs of descaling, indicating calcium loss along the carbonation layer and with the formation of $CaCO_3$ and amorphous silica. Thus, changes in the cement paste microstructure due to amorphous silica precipitation may occur and are considered the most critical concerns in terms of wellbore integrity, since the high porosity material resulting from these processes may allow CO_2 leakage from the reservoir into the atmosphere.

3.2.2. *Cement paste X-Ray porosity and permeability analyses*

X-ray Microtomography analysis (MicroCT) was performed to evaluate the role of BP as an SCM in the macroscopic cement paste properties, before and after the carbonation process caused by the degradation experiments. X-ray microtomography analysis allows the differentiation of cement microconstituents based on the density difference between phases. Denser mineral portions, such as calcium carbonate, are identified as brighter spots, while lighter microconstituents, such as incorporated air or aqueous solution in the pores, are represented as darker spots (Han et al., 2013). MicroCT images from the non-carbonated and carbonated cement specimens are presented in Fig. 5.

From Fig. 5, it can be seen that a low content of basalt powder induces the reduction of specimens' macroporosity and reduces the amount of air incorporated in the material. In the BP 0.25 (Fig. 5B) image, no less-dense spots (darker spots) can be seen, whereas in the BP 0.00 (Fig. 5A) image, there are signs consistent with the presence of large pores, confirming that the addition of BP can reduce the overall porosity of the cement paste. Thus, the reduction in the macroporosity observed in BP 0.25 (Fig. 5B) when compared to the reference (BP 0.00 - Fig. 5A) confirms that the addition of BP refines the porous structure of the cement, increasing the material resistance against the intrusion of

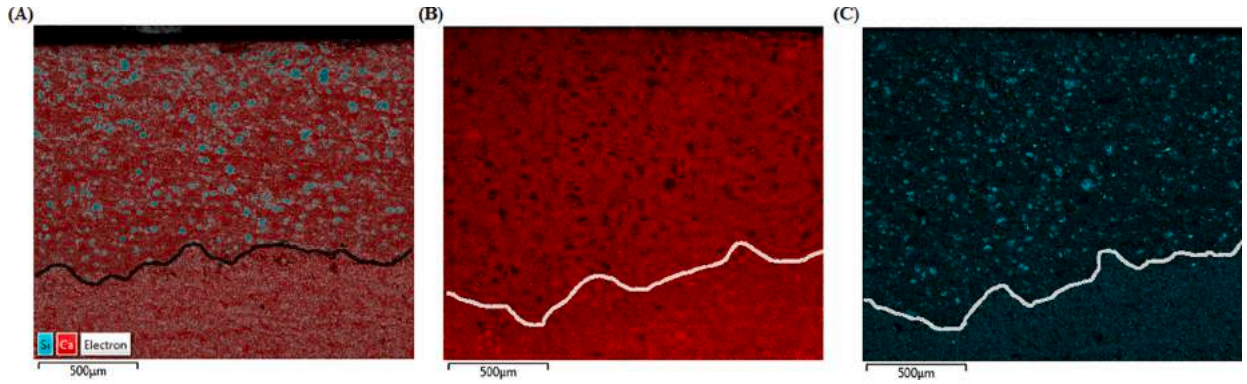

Fig. 4. Elemental distribution in the carbonated layer, dissolution zone and unaltered cement of (A) BP 0.00 (Ca and Si), (B) BP 0.25 (Ca) and (C) BP 0.25 (Si). Ca in red and Si in light green color.

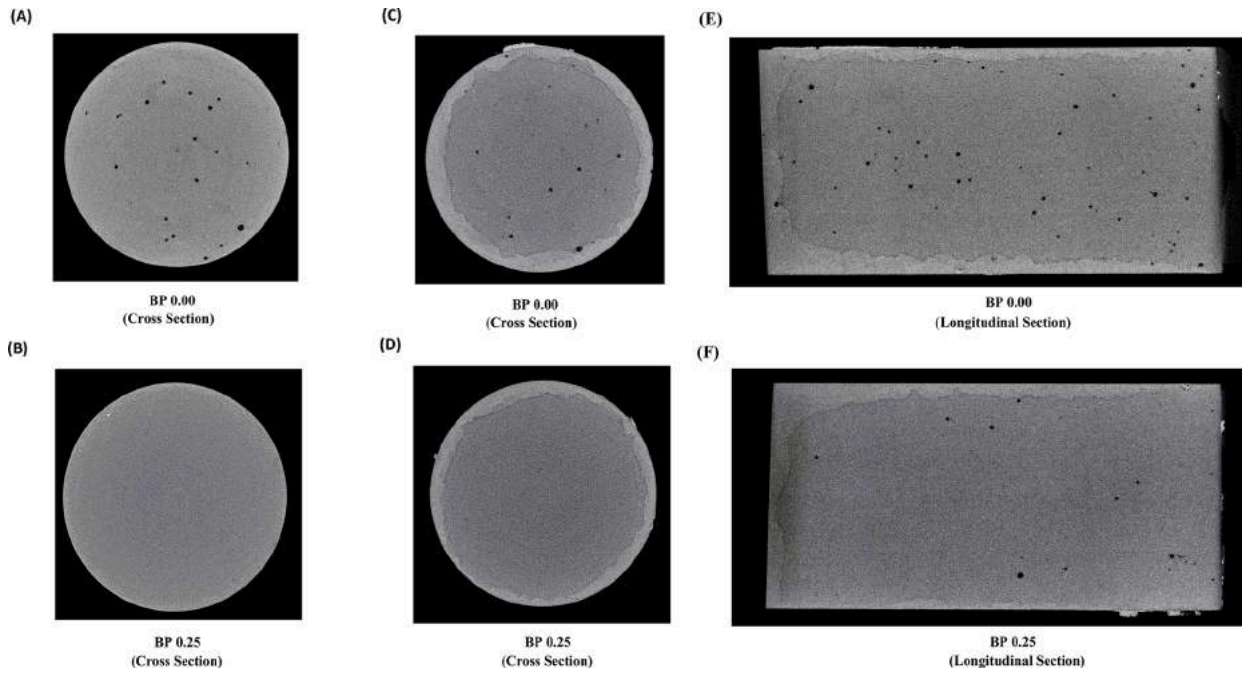

Fig. 5. MicroCT images of cement specimen's cross section before carbonation tests (A) BP 0.00 and (B) BP 0.25, cross section after carbonation tests (C) BP 0.00 and (D) BP 0.25 and longitudinal section after carbonation tests (E) BP 0.00 and (F) BP 0.25.

acidic fluids such as CO_2. For comparison purposes, the MicroCT analysis was performed on the same cement specimens after exposure to CO_2 degradation and the results are also show in Fig. 5C-F.

According to Han et al. (2013), the higher density area (bright grey) is formed after carbonation as a result of portlandite and C-S-H gel transformation into $CaCO_3$, decreasing the permeability by the increase of solid volume and pore filling. From the MicroCT image (Fig. 5C-F), it is possible to notice the effect of carbonation on the cement matrix after the degradation test. The presence of a bright phase on the edge of the cement specimens (not seen in Fig. 5A and 5B) indicates the formation of a denser carbonated layer, resulting from the reaction between CO_2 and cement minerals as the degradation front advances. The extension of the area with higher density (carbonated zone) is more evident in the BP 0.00 specimen than in BP 0.25, indicating that even a small amount of basalt powder can significantly reduce the material's porosity and permeability and increase the cement resistance to CO_2 degradation, as seen in Fig. 5C-F. Therefore, to evaluate these results from different analyses, the carbonated layer thickness estimated by phenolphthalein test, and the carbonated volume measured by the MicroCT analysis, were conducted and the results are shown in Fig. 6.

Fig. 6 shows that the extent of carbonation estimated by both the phenolphthalein method and MicroCT analysis present a reasonable agreement. The microtomography results (Fig. 5) corroborate the phenolphthalein test profiles (Fig. 2), in which the cement pastes with low contents of BP ($\leq$ 0.50 wt.%) present a better performance. The formulations BP 0.25 and BP 0.50 show superior results in terms of resistance against CO_2 degradation when compared to formulations with neat cement paste (BP 0.00) and those formulations with higher BP contents (BP 1.0, BP 2.50, and BP 5.00). Such improvement in the properties of porosity, permeability and chemical resistance to CO_2 is attributed to small additions of BP, since the cement formulations with higher water-to-solids ratio, BP 0.25 (W/S = 0.439) and BP 0.50 (W/S = 0.438), have greater resistance to carbonation than samples with higher density: BP 1.00 (W/S = 0.436), BP 2.50 (W/S = 0.429) and BP 5.00 (W/

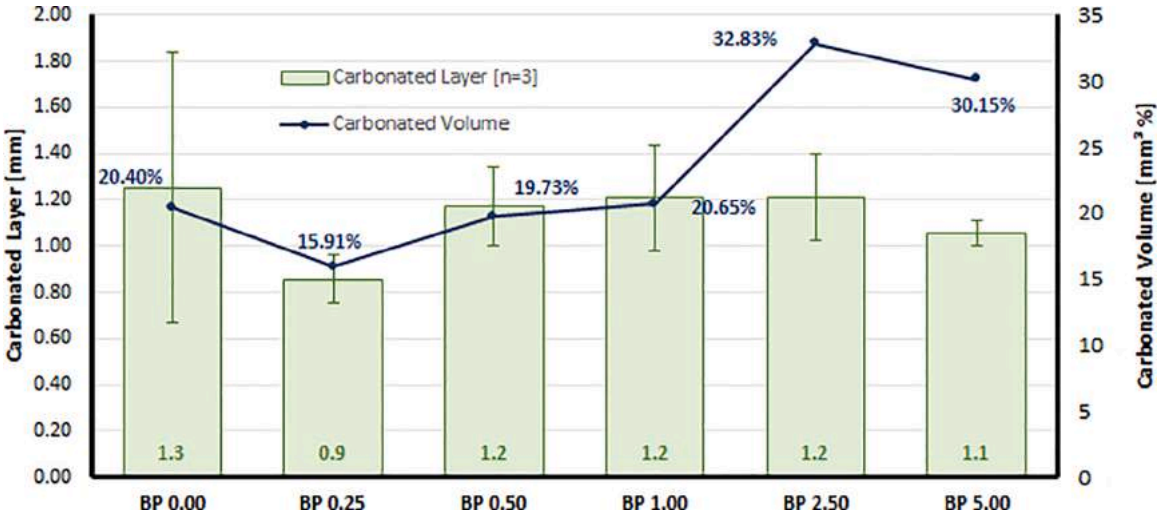

Fig. 6. Carbonated layer thickness (from phenolphthalein test) and carbonated volume (from MicroCT test) of the cement specimens after CO_2 degradation test.

S = 0.419). MicroCT results reinforce the conclusion that the addition of basalt powder at low contents increases the cement paste resistance to the CO_2-rich medium by refining the porous structure and reducing the cement sheath permeability. Thus, to confirm these statements, the porosities of the initial (non-carbonated) and final (carbonated) cement specimens were estimated from the MicroCT data processing and the results are presented in Table 4.

Considering that basalt powder presents slight pozzolanic activity, the decrease in CO_2 degradation resistance shown by specimens with higher levels of BP may be related to increased porosity, reduced alkaline reserve, and increased amount of air incorporated in the cement paste (Uysal and Yilmaz, 2011). Thus, the same characteristics that helps to improve the cement paste performance in formulations with low BP contents ($\leq$ 0.50 wt.%), such as filler character and pore blocking effect, results in an increased porosity and permeability of the cement when it is in high concentrations ($\geq$ 1.00 wt.%). In this way, the low pozzolanic reactivity and the high inert fraction of the basalt powder can lead to a delay in the hydration process, resulting in a fraction of unreacted BP, changing the spacing of the cement matrix and increasing the porosity and permeability of the cement. Furthermore, these characteristics may be influenced by the lower availability of water in formulations with higher basalt powder contents (BP 1.00 - W/S = 0.436; BP 2.50 - W/S = 0.429; BP 5.00 - W/S = 0.419), which should be evaluated in future studies.

From Table 4 it is possible to observe that the porosity of the non-carbonated samples (IP) ranged from 0.08 to 1.06 mm^3 %, while the porosity of the carbonated samples (FP) ranged from 0.08 to 1.28 mm^3 %. As previously discussed, for both samples (carbonated and non-carbonated) there is an initial tendency to reduce porosity, which can be attributed to the basalt powder filler behavior, the pore blocking effect and the consequent refinement of the porous structure of the cement. This characteristic is observed from the reference sample (BP 0.00 – 0.49 mm^3 %) to the BP 0.50 cement specimens (0.08 mm^3 %), which has the lowest initial porosity value among the evaluated formulations. Otherwise, as the BP content increases from BP 0.50 (0.08 mm^3 %) to BP 5.00 (0.35 mm^3 %), the porosity of the cement begins to increase, with a maximum at BP 2.50 cement specimens (1.06 mm^3 %), reflecting the low reactivity of the basalt powder. Regarding the variation in porosity resulting from the carbonation process, a general tendency to reduce the total pore volume is observed. Such a reduction is explained by the pores filling with calcium carbonate resulting from the reaction between CO_2 and portlandite. In this process, $CaCO_3$ acts as an expansive agent, filling the empty space and reducing the porosity and permeability of the cement.

3.3. Mechanical resistance of cement formulations

The influence of basalt powder addition on the mechanical strength of the cement formulations was evaluated both before and after the carbonation process. Compressive strength after carbonation process is an important property to be measured, since calcium carbonate precipitation can positively influence the cement paste porosity at the beginning of the degradation process (Bertos et al., 2004; Kutchko et al., 2007; Ledesma et al., 2020; Rochelle et al., 2004). The results of compressive strength are detailed in Table 5.

From Table 5 it can be seen that the compressive strength of the non-carbonated samples ranged from 23.7 to 57.7 MPa, while the compressive strength of the carbonated samples ranged from 33.7 to 52.7 MPa. In addition, it is well known that porosity can influence both the microscopic (in this case study, CO_2 diffusivity) and macroscopic properties, such as the compressive strength of a cementitious material. Thus, to improve data interpretation, mechanical resistance results were plotted together with porosity data of the cement specimens and the results are shown in Fig. 7. The results of the mechanical and micro-tomography tests were obtained from cement specimens from the same batch, being the samples (carbonated and non-carbonated) prepared at the same time.

From Fig. 7, it is possible to observe a positive effect of basalt powder on the initial compressive strength of cement specimens with high BP contents ($\geq$ 0.50 wt.%), despite the increase in porosity. For both samples (non-carbonated and carbonated) there is an initial increase in compressive strength, with the maximum being obtained for the sample with 0.50 wt.% of basalt powder (BP 0.50). This is followed by a reversal in the trend for the cement specimens with high BP contents and low water-to solids ratios (BP 1.00 - W/S = 0.436; BP 2.50 - W/S = 0.429; BP 5.00 - W/S = 0.419). Regarding the influence of carbonation on the cement's mechanical properties, only for samples with low basalt powder content and high water-to solids ratios (BP 0.25 - W/S = 0.439; BP 0.50 - W/S = 0.438) the final compressive strength (carbonated samples) was higher than that initially measured (non-carbonated samples). Otherwise, the loss in the mechanical strength is clearly seen for samples with high contents of basalt powder (BP 1.00, BP 2.50, and BP 5.00), since the final compressive strength is lower than that measured before the carbonation process. As previously discussed, the low pozzolanic reactivity and the high inert fraction of the basalt powder can lead to a delay in the hydration process, resulting in unreacted BP fraction, changing the spacing of the cement matrix and resulting on an increased porosity and permeability of the cement formulations with high contents of basalt powder (BP 1.00, BP 2.50, and BP 5.00). These modifications in the cement structure increase degradation by CO_2 and reduce mechanical properties of the cement after carbonation. Furthermore, these characteristics may be influenced by the low availability of water in formulations with high basalt powder content (BP 1.00 - W/S = 0.436; BP 2.50 - W/S = 0.429; BP 5.00 - W/S = 0.419), which should be evaluated in future studies.

Even though BP 0.25 has the greater carbonation resistance (Fig. 6), it presents a similar behavior of compressive strength, both before and after carbonation, to that obtained for the reference sample (BP 0.00). For both specimens (BP 0.00 and BP 0.25), after carbonation, the increase in compressive strength is accompanied by a reduction in the porosity. Furthermore, BP 0.50 has the highest compressive strength, which is slightly compromised by the carbonation process, and the lowest porosity value, that is practically unchanged by the degradation process. Thus, it can be concluded that low basalt content in the cement paste can modify the cement's microstructural properties, such as porosity, for example. However, these changes are not enough to

Table 4
Porosity of cement formulations with basalt powder, before (initial) and after (final) carbonation.

Sample	BP [wt.%]	W/S	IP [mm^3 %]	FP [mm^3 %]
BP 0.00	0.00	0.440	0.49	0.40
BP 0.25	0.25	0.439	0.12	0.08
BP 0.50	0.50	0.438	0.08	0.08
BP 1.00	1.00	0.436	0.66	0.60
BP 2.50	2.50	0.429	1.06	1.28
BP 5.00	5.00	0.419	0.35	0.29

BP - Basalt Powder; W/S – Water-to-Solids Ratio; IP - Initial Porosity; FP - Final Porosity.

Table 5
Compressive strength of cement formulations with basalt powder, before (initial) and after (final) carbonation.

Sample	BP [wt.%]	W/S	IC [MPa]	FC [MPa]
BP 0.00	0.00	0.440	28.0 ± 3.6	42.0 ± 8.9
BP 0.25	0.25	0.439	23.7± 3.1	45.3 ± 7.5
BP 0.50	0.50	0.438	57.7 ± 4.2	52.7 ± 18.8
BP 1.00	1.00	0.436	50.7 ± 13.6	40.0 ± 4.0
BP 2.50	2.50	0.429	42.3 ± 5.0	42.7 ± 2.4
BP 5.00	5.00	0.419	45.7 ± 10.2	33.7 ± 11.4

BP - Basalt Powder; W/S – Water-to-Solids Ratio; IC - Initial Compression; FC - Final Compression.

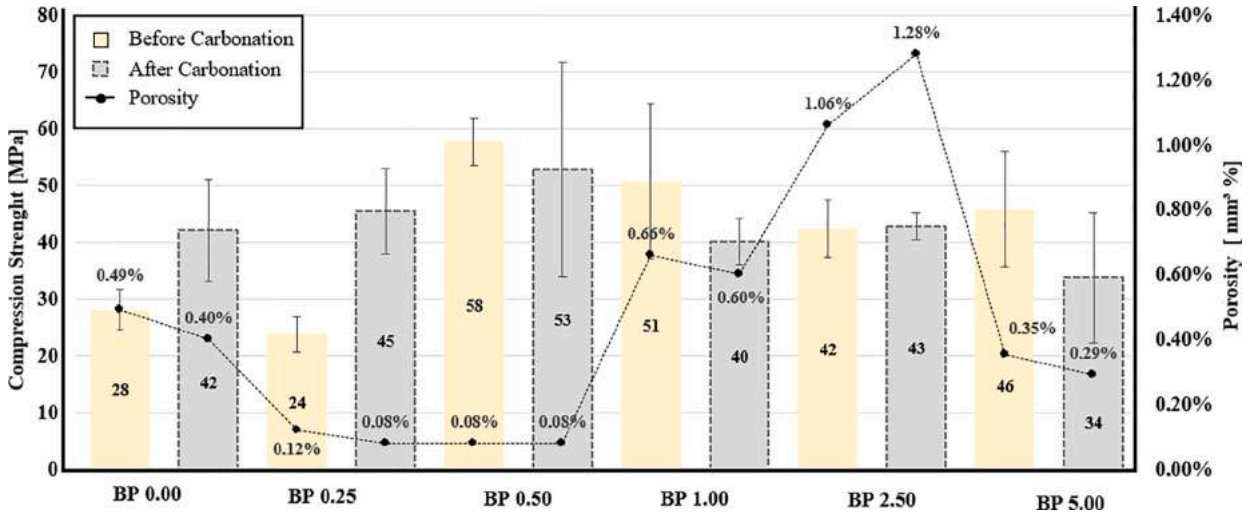

Fig. 7. Porosity and compressive strength of cement formulations with basalt powder, before and after carbonation.

promote significant differences in the material's macrostructural properties, such as compressive strength. Otherwise, the BP 1.00, BP 2.50 and BP 5.00 cement formulations have a significant loss of compressive strength after the carbonation process (less pronounced for BP 2.50), while having porosity values substantially higher than the reference sample (BP 0.00). Although calcium carbonate can fill the pores and reduce the cement porosity, the larger pores cannot be completely filled. Thus, the porosity can be reduced with no significant changes in the mechanical strength. This behavior can be seen by comparing Fig. 5A and Fig. 5C, in which the small pores are filled while the larger pores remain apparently unchanged.

Contrary to the literature, our results show that the formation of a carbonated layer (with higher density) and of a dissolution zone (with high porosity) in the cement paste promotes the loss of the material's integrity since it creates a preferential fracture plane delimited by the interface between the degraded and unaltered zones. In addition, this process, among other factors such as changes in total porosity, can influence the results of compressive strength after carbonation because the detachment of the carbonated layer decreases the cross-section area of the specimen and consequently decreases its compressive resistance. This behavior is shown in Figure S4 (Supplementary Material) and was observed during the compressive strength analysis for all the cement specimens submitted to carbonation process in which the detachment of the carbonated layer (grey zone), along with a preferential cleavage plane, clearly exposed the unreacted cement core (pink zone).

Thus, in addition to the integrity loss, the difference in mechanical and elastic properties between the carbonated and non-carbonated layers can lead to the formation of cracks and preferential paths for fluids percolation. Thus, the degradation process can be accelerated due to the formation of paths with less resistance to the intrusion of acidic fluids in the cement matrix, which can lead to catastrophic failure of the well. Considering that the CO_2 degradation front is not homogeneous (Fig. 4), and that there is a preferential fracture plane delimited by the interface between the degraded and unaltered zones (Figure S4), it is recommended in future studies to perform mechanical tests in different portions of the cross section of the specimens through microindentation hardness tests in order to evaluate how the mechanical resistance is modified along the different phases of the material (carbonated, intermediates and unaltered cement zones).

3.4. Data analysis

After the comprehensive study on the chemical, mechanical and microstructural properties of cement formulations with basalt powder, data analysis was applied to analyze the correlation between the measured variables and the basalt content added to the formulations. In the present work, data analysis was performed using Correlation Analysis (CA) and the multivariate analysis methods Principal Component analysis (PCA), and Hierarchical Clustering Analysis (HCA), using the basalt powder content (BP), water-to-solids ratio (W/S), carbonated layer (CL), carbonated volume (CV), initial porosity (IP), final porosity (FP), initial compressive strength (IC), and final compressive strength (FC), already presented in Tables 3-5. For brevity, only the most important correlations are discussed, however, numerical linear relationship results among the parameters are detailed in Table S1 in the Supplementary Material. Results of the PCA and HCA analyses are shown in Fig. 8, while the results of the correlation analysis are presented in the Supplementary Material (Table S1 and Figure S5).

Through PCA analysis, the most relevant data (explained variance) is recovered and represented by the Score (sample projection) and Loading (variable influence) graphics. From the PCA results (Fig. 8A), only two principal components (PC 1 - 50.80% and PC 2 - 25.06%) represent 75.86% of the data set explained variance. From the PCA (Fig. 8A), it is observed that the reference sample (BP 0.00) and the formulations with low basalt power contents (BP 0.25 and BP 0.50) are shifted to negative PC-1 values, while the formulations with high BP contents (BP 1.00, BP 2.50, and BP 5.00) are shifted to positive PC-1 values. From the loadings and sample position along the PC-1 axis, formulations with high basalt powder content (BP 1.00, BP 2.50, and BP 5.00) and low water-to-solids ratio (W/S) are associated with higher values of initial compressive strength (IC), carbonated layer (CL), carbonated volume (CV), initial (IP) and final porosity (FP). Thus, from the PCA loadings, it can be observed that the formulations displaced to positive values of PC-1 presented less chemical resistance to CO_2 than the reference sample (BP 0.00). Otherwise, the cement formulations with low basalt powder content (BP 0.25 and BP 0.50) and high water-to-solids ratio (W/S) are shifted to negative PC-1 values and present a higher final compressive strength (FC) and lower carbonated fraction (CL and CV) and porosity (IP and FP) than the reference specimens (BP 0.00).

Although both formulations (BP 0.25 and BP 0.50) perform better than the reference sample against CO_2 degradation, from the PC-2 scores and loadings, we found that the formulation with 0.25 wt.% of BP presents a higher chemical resistance, while the formulation with 0.50 wt.% of BP has better mechanical performance. These characteristics allow the new cement formulations to be applied in different extensions of the well construction. Thus, BP 0.25 could be applied in extensions where issues related to chemical resistance to CO_2 are more important, while BP 0.50 could be used in well extensions that are subject to greater

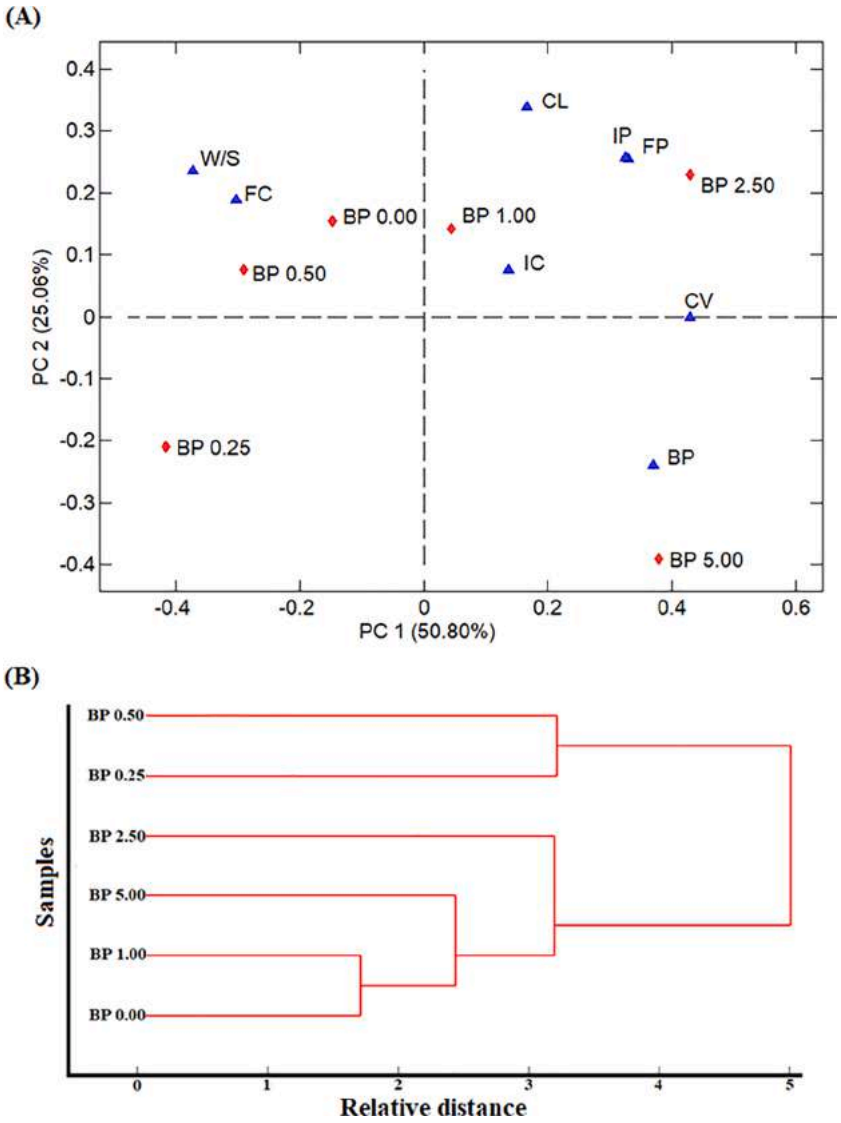

Fig. 8. Data analysis of cement formulations with addition of basalt powder, before and after carbonation: (A) PCA and (B) HCA.

mechanical stress. These characteristics are reinforced by the HCA dendrogram (Fig. 8B) in which the formulations BP 0.25 and BP 0.50 have a set of properties that significantly distinguish them from the others (BP 0.00, BP 1.00, BP 2.50, and BP 5.00) and clearly indicate their better performance in aggressive environments.

From the correlation analysis (Figure S5 and Table S1), a significant positive relationship between basalt powder (BP) content and carbonated volume of the cement formulations (R^2 = 0.82) was identified, while there is a significant negative relationship between the BP content and the final compressive strength (R^2 = -0.71) of the cement specimens. Furthermore, a slightly positive relationship was observed between BP and the initial porosity (R^2 = 0.25), final porosity (R^2 = 0.26) and initial compressive strength (R^2 = 0.30), while there is a fairly positive adjustment between the initial porosity and the carbonated layer (R^2 = 0.56) and carbonated volume (R^2 = 0.67). Thus, we may conclude that high contents of basalt powder in the cement formulations lead to an increase in the material porosity which favors the carbonation process, modifying the cement microstructure and compromising the mechanical and chemical integrity of the material throughout the carbonation process. Thus, only small additions of BP ($\leq$ 0.5 wt.%) in the formulations are beneficial to increase the chemical resistance of the cement against CO_2.

In addition, from the correlation analysis (Figure S5 and Table S1), significant positive relationship between the water-to-solids ratio (W/S) and final compression strength (R^2 = 0.71) was identified, while there is significant negative relationship between the W/S and the carbonated volume (R^2 = -0.82) of the cement specimens. Furthermore, slightly negative relationship was observed between W/S and the initial porosity (R^2 = -0.26), final porosity (R^2 = -0.27) and initial compressive strength (R^2 = -0.30). The literature argues that cement formulations with lower water-to-solids ratio are expected to have greater resistance to carbonation (Costa et al., 2019; Torsaeter et al., 2013). However, from the data analysis, we identified that the samples with the higher W/S and lower BP content (BP 0.25 and BP 0.50) showed the best resistance against CO_2. Thus, it can be concluded that these formulations balance the properties of the cement formulations from pore filling with basalt powder without impairing the curing process and significantly change the density of the cement paste. On the other hand, the low pozzolanic reactivity and the high inert fraction of the basalt powder can lead to a delay in the hydration process, resulting in an unreacted BP fraction, changing the spacing of the cement matrix and increasing the porosity and permeability of the cement formulations with higher contents of basalt powder (BP 1.00, BP 2.50, and BP 5.00). These modifications of the cement structure increase degradation by CO_2 and reduce the cement mechanical properties after carbonation. From these results, it is observed that future studies should also evaluate the influence of the

water-to-solids ratio (W/S) on the chemical and mechanical resistance properties of cement formulations with basalt powder.

From the data analysis we conclude that formulations with a low content of basalt powder (BP 0.25 and BP 0.50) are those with the greatest potential for application in CCS wells. Both formulations have low initial porosity and maintain their mechanical properties, even after the carbonation process. While the formulation with 0.25 wt.% of basalt powder (BP 0.25) has greater chemical resistance, being recommended for application in well extensions exposed to more aggressive environments, the formulation with 0.50 wt.% of basalt powder (BP 0.50) would be preferred for a well session subject to moderate CO_2 activity, but which requires materials with high mechanical resistance. Furthermore, considering that the addition of BP is small ($\leq$ 0.5 wt.%), the impacts on the production cost of these cement formulations could be easily compensated by the increase in the well integrity and the extension of its life cycle.

3.5. Financial assessment of BP addition to cement paste

In this topic, the financial assessment of BP addition to the cement paste is provided. The base-price used in the assessment for class G cement was $ 0.27 US dollar (R$ 1.49) per kg, informed by Lafarge Holcim Brazil (base year 2019). The coarse aggregate price was $ 8.65 US dollar (R$ 47.00) per cubic meter (m^3), obtained from the Brazilian civil construction report of SINAPI (price and cost references - July 2020) (SINAPI, 2020). Thus, Fig. 9 shows a comparison of the cost per m^3 of the proposed new well cement formulations with the addition of mass fractions of basalt powder (from 0.25 to 5 wt.%).

Financial assessment (Fig. 9) shows a tendency for a slight increase in formulation costs as the basalt powder fraction is increased from 0 to 5 wt.%. The formulation cost increasing ranges from $ 0.02 US dollar (BP 0.25) to $ 0.44 US dollar (BP 5.00) per metric ton (m^3) of well cement formulation. From the financial assessment and considering the formulations with lower basalt powder contents (BP 0.25 and BP 0.50), which performed better properties in CO_2-rich environment, we can conclude that the cost increase would be easily compensated by the wellbore integrity increase in long term. Thus, formulations that showed better chemical (BP 0.25) and mechanical (BP 0.50) resistances presented insignificant additional costs (per m^3) in relation to the reference cement formulation (Class G cement - BP 0.00), attesting that BP can be a low-cost SCM with interesting cost/benefit relationship to be applied in chemical-resistant cement formulation for CCS wells.

4. Conclusions

In the present work, we propose the application of basalt powder (BP) as a supplementary cementitious material (SCM) in cement formulations for Carbon Capture and Storage (CCS) wells. From the experimental results, we identified that BP can be characterized as a filled-pozzolanic SCM, since it has low pozzolanic activity, large inert fraction, and particle size significantly smaller than class G cement. The cement formulations (BP + class G cement) were obtained from a simple dry blending process and, within the range of evaluated BP (0.25 to 5.00 wt.%), no significant changes were identified in the characteristics of the fresh cement paste. After curing, the cement specimens were subjected to degradation tests under reservoir conditions (65°C and 15 MPa of CO_2) and a comprehensive characterization of the cement formulations, before and after the carbonation, was performed.

From our results, we identified that the basalt powder can be used as an SCM in cement paste, modifying the fundamental material properties such as microstructure (porosity and permeability), mechanical, and chemical resistance. From the carbonation test results we identified that formulations with low basalt powder content ($\leq$ 0.5 wt.%) and high water-to-solids ratio (W/S) are those with the greatest potential for application in CCS wells, since they are more resistant to CO_2 degradation, present low porosity, and have suitable mechanical properties. Otherwise, formulations with a high BP content ($\geq$ 0.5 wt.%) demonstrated characteristics that may not recommend their application in CCS wells since they presented high porosity, low resistance to CO_2, and mechanical properties that were compromised by the carbonation process.

Due to the characteristics of the basalt powder (filled-pozzolanic SCM with high surface area and small particle size) we conclude that the increase shown in chemical resistance for cement formulations with low BP contents ($\leq$ 0.5 wt.%) is due to the reduction of material porosity and permeability, the filling of empty spaces, and refinement of the porous cement network together with the low reduction of the alkaline reserve of portlandite. These combined features increased the class G cement paste's resistance to fluid intrusion, delayed the progress of the CO_2 degradation front, and preserved the cement matrix's ability to neutralize acid gases. Thus, from our results, we conclude that addition of BP to cement formulations at low contents can improve the CCS well integrity and extend its life cycle.

For the application of the BP technology in a full-scale wellbore, properties such as: (*i*) thickening time, (*ii*) free water content, (*iii*) fluid

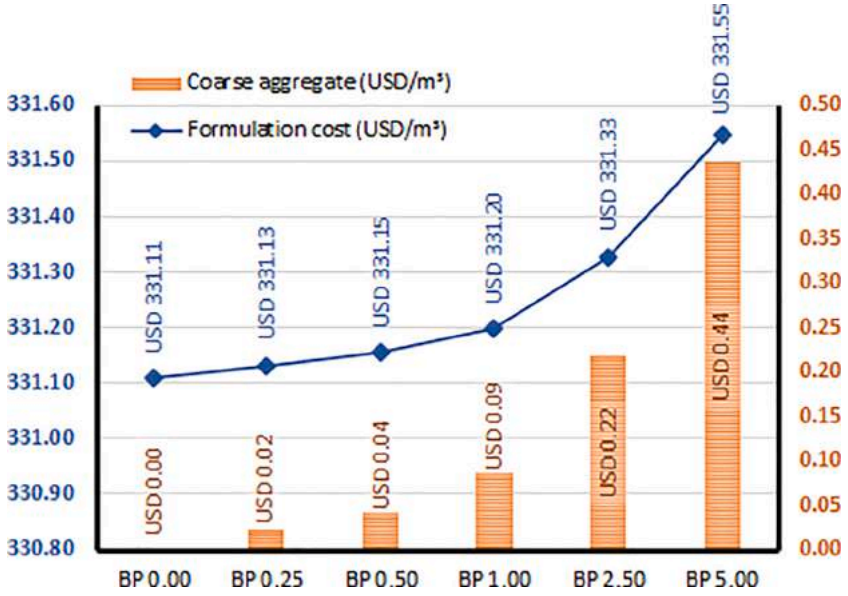

Fig. 9. Financial assessment of formulations with basalt powder.

loss and (*iv*) rheology, as well as the need of additional additives (i.e., anti-foam, retardant, and dispersant) must be evaluated in future studies to ensure that the new formulations meet the wide range specifications of CCS projects. Furthermore, additional studies should be carried out to evaluate the influence of the water-to-solids ratio (W/S) on the chemical and mechanical resistance properties of cement formulations with basalt powder.

CRediT authorship contribution statement

Gabriela Gonçalves Dias Ponzi: Conceptualization, Methodology, Validation, Formal analysis, Investigation, Data curtion, Writing – original draft, Writing – review & editing, Visualization. **Victor Hugo Jacks Mendes dos Santos:** Conceptualization, Methodology, Software, Validation, Formal analysis, Investigation, Data curtion, Writing – original draft, Writing – review & editing, Visualization. **Renan Bordulis Martel:** Methodology, Validation, Formal analysis. **Darlan Pontin:** Conceptualization, Methodology, Validation, Formal analysis, Investigation. **Amanda Sofia de Guimarães e Stepanha:** Methodology, Validation, Formal analysis. **Marta Kerber Schütz:** Conceptualization, Methodology, Validation, Formal analysis, Investigation, Data curtion, Writing – original draft, Writing – review & editing, Visualization. **Sonia C. Menezes:** Conceptualization, Methodology, Validation, Investigation, Resources, Data curtion, Supervision, Project administration, Funding acquisition. **Sandra M.O. Einloft:** Conceptualization, Methodology, Validation, Investigation, Resources, Data curtion, Supervision, Project administration, Funding acquisition. **Felipe Dalla Vecchia:** Conceptualization, Methodology, Software, Validation, Formal analysis, Investigation, Resources, Data curtion, Writing – original draft, Writing – review & editing, Visualization, Supervision, Project administration, Funding acquisition.

Declaration of Competing Interest

The authors declare that they have no known competing financial interests or personal relationships that could have appeared to influence the work reported in this paper.

Acknowledgments

The authors would like to thank the Institute of Petroleum and Natural Resource (IPR) of the Pontifical Catholic University of Rio Grande do Sul for the infrastructure, the Coordination for the Improvement of Higher Education Personnel (CAPES) for the research scholarships and Lafarge Holcim for the donation of the cement. This work was supported by Petrobras (grant numbers: 2017/00742-8 and 2018/00235-1) and by ANP (Brazil's National Oil, Natural Gas and Biofuels Agency), through the R&D levy regulation.

Supplementary materials

Supplementary material associated with this article can be found, in the online version, at doi:10.1016/j.ijggc.2021.103337.

References

Abid, K., Gholami, R., Elochukwu, H., Mostofi, M., Bing, C.H., Muktadir, G., 2018. A methodology to improve nanosilica based cements used in CO_2 sequestration sites. Petroleum 4, 198–208. https://doi.org/10.1016/j.petlm.2017.10.005.

Abid, K., Gholami, R., Mutadir, G., 2020. A pozzolanic based methodology to reinforce Portland cement used for CO_2 storage sites. J. Nat. Gas Sci. Eng. 73 https://doi.org/10.1016/j.jngse.2019.103062.

ABNT, 2010. NBR 15895 - Materiais pozolânicos – Determinação do teor de hidróxido de cálcio fixado – Método Chapelle modificado. Assoc. Bras. Normas Técnicas 1–10 https://doi.org/01.080.10; 13.220.99.

API Specification, 2010. API 10A - Specification for Cements and Materials for Well Cementing. Am. Pet. Inst. 2009, 50. https://doi.org/10.1002/jcc.

API Specification, 2000. API 10B - Recommended pratice for testing well cements. Am. Pet. Inst. 1–151.

Ashraf, W., 2016. Carbonation of cement-based materials: Challenges and opportunities. Constr. Build. Mater. 120, 558–570. https://doi.org/10.1016/j.conbuildmat.2016.05.080.

ASTM International, 2018. ASTM C39 - Standard Test Method for Compressive Strength of Cylindrical Concrete Specimens. ASTM Stand. West Conshohocken 1–8. https://doi.org/10.1520/C0039.

Bagheri, M., Shariatipour, S.M., Ganjian, E., 2018. A review of oil well cement alteration in CO_2-rich environments. Constr. Build. Mater. 186, 946–968. https://doi.org/10.1016/j.conbuildmat.2018.07.250.

Bai, M., Sun, J., Song, K., Li, L., Qiao, Z., 2015. Well completion and integrity evaluation for CO_2 injection wells. Renew. Sustain. Energy Rev. 45, 556–564. https://doi.org/10.1016/j.rser.2015.02.022.

Bai, M., Zhang, Z., Fu, X., 2016. A review on well integrity issues for CO_2 geological storage and enhanced gas recovery. Renew. Sustain. Energy Rev. 59, 920–926. https://doi.org/10.1016/j.rser.2016.01.043.

Baldissera, A.F., Schütz, M.K., dos Santos, L.M., Vecchia, F.D., Seferin, M., Ligabue, R., Costa, E.M., Chaban, V.V., Menezes, S.C., Einloft, S., 2017a. Epoxy resin-cement paste composite for wellbores: Evaluation of chemical degradation fostered carbon dioxide. Greenh. Gases Sci. Technol. 7, 1065–1079. https://doi.org/10.1002/ghg.1700.

Baldissera, A.F., Schütz, M.K., Vecchia, F.D., Seferin, M., Ligabue, R., Menezes, S.C., Einloft, S., 2017b. Epoxy-modified Portland Cement: Effect of the Resin Hardener on the Chemical Degradation by Carbon Dioxide. Energy Procedia 114, 5256–5265. https://doi.org/10.1016/j.egypro.2017.03.1682.

Benezet, J.C., Benhassaine, A., 1999. Grinding and pozzolanic reactivity of quartz powders. Powder Technology. https://doi.org/10.1016/S0032-5910(99)00133-3.

Bertos, M.F., Simons, S.J.R., Hills, C.D., Carey, P.J., 2004. A review of accelerated carbonation technology in the treatment of cement-based materials and sequestration of CO_2. J. Hazard. Mater. 112, 193–205. https://doi.org/10.1016/j.jhazmat.2004.04.019.

Bjørge, R., Gawel, K., Chavez Panduro, E.A., Torsæter, M., 2019. Carbonation of silica cement at high-temperature well conditions. Int. J. Greenh. Gas Control 82, 261–268. https://doi.org/10.1016/j.ijggc.2019.01.011.

Borges, P.H.R., Costa, J.O., Milestone, N.B., Lynsdale, C.J., Streatfield, R.E., 2010. Carbonation of CH and C–S–H in composite cement pastes containing high amounts of BFS. Cem. Concr. Res. 40, 284–292. https://doi.org/10.1016/j.cemconres.2009.10.020.

Carey, J.W., Wigand, M., Chipera, S.J., WoldeGabriel, G., Pawar, R., Lichtner, P.C., Wehner, S.C., Raines, M.A., Guthrie, G.D., 2007. Analysis and performance of oil well cement with 30 years of CO_2 exposure from the SACROC Unit, West Texas, USA. Int. J. Greenh. Gas Control 1, 75–85. https://doi.org/10.1016/S1750-5836(06)00004-1.

Carroll, S., Carey, J.W., Dzombak, D., Huerta, N.J., Li, L., Richard, T., Um, W., Walsh, S.D.C., Zhang, L., 2016. Review: Role of chemistry, mechanics, and transport on well integrity in CO_2 storage environments. Int. J. Greenh. Gas Control 49, 149–160. https://doi.org/10.1016/j.ijggc.2016.01.010.

Costa, B.L., de, S., Freitas, J.C., de, O., Melo, D.M., de, A., Araujo, R.G., da, S., Oliveira, Y.H.de, Simão, C.A., 2019. Evaluation of density influence on resistance to carbonation process in oil well cement slurries. Constr. Build. Mater. 197, 331–338. https://doi.org/10.1016/j.conbuildmat.2018.11.232.

De Sena Costa, B.L., de Oliveira Freitas, J.C., Silva Santos, P.H., Gomes da Silva Araújo, R., dos Santos Oliveira, J.F., de Araújo Melo, D.M., 2018. Study of carbonation in a class G Portland cement matrix at supercritical and saturated environments. Constr. Build. Mater. 180, 308–319. https://doi.org/10.1016/j.conbuildmat.2018.05.287.

Dobiszewska, M., Beycioğlu, A., 2017. Investigating the Influence of Waste Basalt Powder on Selected Properties of Cement Paste and Mortar. IOP Conf. Ser. Mater. Sci. Eng. 245, 022027 https://doi.org/10.1088/1757-899X/245/2/022027.

Dong, X., Duan, Z., Gao, D., 2020. Assessment on the cement integrity of CO_2 injection wells through a wellbore flow model and stress analysis. J. Nat. Gas Sci. Eng. 74, 103097 https://doi.org/10.1016/j.jngse.2019.103097.

Duguid, A., Radonjic, M., Scherer, G.W., 2011. Degradation of cement at the reservoir/cement interface from exposure to carbonated brine. Int. J. Greenh. Gas Control 5, 1413–1428. https://doi.org/10.1016/j.ijggc.2011.06.007.

El-Didamony, H., Helmy, I.M., Osman, R.M., Habboud, A.M., 2015. Basalt as Pozzolana and Filler in Ordinary Portland Cement. Am. J. Eng. Appl. Sci. 8, 263–274. https://doi.org/10.3844/ajeassp.2015.263.274.

Ghafari, E., Feys, D., Khayat, K., 2016. Feasibility of using natural SCMs in concrete for infrastructure applications. Constr. Build. Mater. 127, 724–732. https://doi.org/10.1016/j.conbuildmat.2016.10.070.

Han, J., Sun, W., Pan, G., 2013. X-ray microtomography of the carbonation front shape evolution of cement mortar and modeling of accelerated carbonation reaction. J. Wuhan Univ. Technol. Sci. Ed. 28, 303–308. https://doi.org/10.1007/s11595-013-0683-8.

Hassaan, M., 2001. Basalt rock as an alternative raw material in Portland cement manufacture. Mater. Lett. 50, 172–178. https://doi.org/10.1016/S0167-577X(01)00220-8.

Iglesias, R.S., Ketzer, J.M., Melo, C.L., Heemann, R., Machado, C.X., 2015. Carbon capture and geological storage in Brazil: an overview. Greenh. Gases Sci. Technol. 5, 119–130. https://doi.org/10.1002/ghg.1476.

Ismail, A.H., Kusbiantoro, A., Chin, S.C., Muthusamy, K., Islam, M., Tee, K.F., 2020. Pozzolanic reactivity and strength activity index of mortar containing palm oil clinker pretreated with hydrochloric acid. J. Clean. Prod. 242, 118565 https://doi.org/10.1016/j.jclepro.2019.118565.

Iyer, J., Walsh, S.D.C., Hao, Y., Carroll, S.A., 2018. Assessment of two-phase flow on the chemical alteration and sealing of leakage pathways in cemented wellbores. Int. J. Greenh. Gas Control 69, 72–80. https://doi.org/10.1016/j.ijggc.2017.12.001.

Jadid, K.M., Okandan (Supervisor), E., 2011. Chemical alteration of oil well cement with basalt additive during carbon storage application. Master Thesis. Middle East Technical University.

Jobard, E., Sterpenich, J., Pironon, J., Corvisier, J., Randi, A., 2018. Experimental Modelling of the Caprock/Cement Interface Behaviour under CO_2 Storage Conditions: Effect of Water and Supercritical CO_2 from a Cathodoluminescence Study. Geosciences 8, 185. https://doi.org/10.3390/geosciences8050185.

Ketzer, J.M., Iglesias, R., Einloft, S., Dullius, J., Ligabue, R., de Lima, V., 2009. Water-rock-CO_2 interactions in saline aquifers aimed for carbon dioxide storage: Experimental and numerical modeling studies of the Rio Bonito Formation (Permian), southern Brazil. Appl. Geochemistry 24, 760–767. https://doi.org/10.1016/j.apgeochem.2009.01.001.

Kiran, R., Teodoriu, C., Dadmohammadi, Y., Nygaard, R., Wood, D., Mokhtari, M., Salehi, S., 2017. Identification and evaluation of well integrity and causes of failure of well integrity barriers (A review). J. Nat. Gas Sci. Eng. 45, 511–526. https://doi.org/10.1016/j.jngse.2017.05.009.

Koukouzas, N., Kypritidou, Z., Vasilatos, C., Tsoukalas, N., Rochelle, C.A., Purser, G., 2017. Geochemical modeling of carbonation of hydrated oil well cement exposed to CO_2-saturated brine solution. Appl. Geochemistry 85, 35–48. https://doi.org/10.1016/j.apgeochem.2017.08.002.

Kutchko, B.G., Strazisar, B.R., Dzombak, D.A., Lowry, G.V., Thauiow, N., Thaulow, N., 2007. Degradation of well cement by CO_2 under geologic sequestration conditions. Environ. Sci. Technol. 41, 4787–4792. https://doi.org/10.1021/es062828c.

Kutchko, B.G., Strazisar, B.R., Lowry, G.V., Dzombak, D.A., Thaulow, N., 2008. Rate of CO_2 Attack on Hydrated Class H Well Cement under Geologic Sequestration Conditions. Environ. Sci. Technol. 42, 6237–6242. https://doi.org/10.1021/es800049r.

Kuzielová, E., Žemlička, M., Másilko, J., Palou, M.T., 2018. Effect of additives on the performance of Dyckerhoff cement, Class G, submitted to simulated hydrothermal curing. J. Therm. Anal. Calorim. 133, 63–76. https://doi.org/10.1007/s10973-017-6806-2.

Labbaci, Y., Abdelaziz, Y., Mekkaoui, A., Alouani, A., Labbaci, B., 2017. The use of the volcanic powders as supplementary cementitious materials for environmental-friendly durable concrete. Constr. Build. Mater. 133, 468–481. https://doi.org/10.1016/j.conbuildmat.2016.12.088.

Laibao, L., Yunsheng, Z., Wenhua, Z., Zhiyong, L., Lihua, Z., 2013. Investigating the influence of basalt as mineral admixture on hydration and microstructure formation mechanism of cement. Constr. Build. Mater. 48, 434–440. https://doi.org/10.1016/j.conbuildmat.2013.07.021.

Lavrov, A., 2018. Stiff cement, soft cement: Nonlinearity, arching effect, hysteresis, and irreversibility in CO_2-well integrity and near-well geomechanics. Int. J. Greenh. Gas Control 70, 236–242. https://doi.org/10.1016/j.ijggc.2017.11.012.

Ledesma, R.B., Lopes, N.F., Bacca, K.G., Moraes, M.K.de, Batista, G.dos S., Pires, M.R., Costa, E.M.da, 2020. Zeolite and fly ash in the composition of oil well cement: Evaluation of degradation by CO_2 under geological storage condition. J. Pet. Sci. Eng. 185, 106656 https://doi.org/10.1016/j.petrol.2019.106656.

Liu, C., Liu, G., Liu, Z., Yang, L., Zhang, M., Zhang, Y., 2018. Numerical simulation of the effect of cement particle shapes on capillary pore structures in hardened cement pastes. Constr. Build. Mater. 173, 615–628. https://doi.org/10.1016/j.conbuildmat.2018.04.039.

Lorek, A., Labus, M., Bujok, P., 2016. Wellbore cement degradation in contact zone with formation rock. Environ. Earth Sci. 75, 499. https://doi.org/10.1007/s12665-015-5114-z.

Lothenbach, B., Scrivener, K., Hooton, R.D., 2011. Supplementary cementitious materials. Cem. Concr. Res. 41, 1244–1256. https://doi.org/10.1016/j.cemconres.2010.12.001.

Mahmoud, A.A., Elkatatny, S., 2019. Mitigating CO_2 reaction with hydrated oil well cement under geologic carbon sequestration using nanoclay particles. J. Nat. Gas Sci. Eng. 68 https://doi.org/10.1016/j.jngse.2019.102902.

Metz, B., Davidson, O., De Coninck, H., Loos, M., Meyer, L., 2005. IPCC special report on carbon dioxide capture and storage. Intergovernmental Panel on Climate Change.

Moosakazemi, F., Tavakoli Mohammadi, M.R., Mohseni, M., Karamoozian, M., Zakeri, M., 2017. Effect of design and operational parameters on particle morphology in ball mills. Int. J. Miner. Process. 165, 41–49. https://doi.org/10.1016/j.minpro.2017.06.001.

Mosleh, M.H., Durucan, S., Syed, A., Shi, J.-Q.Q., Korre, A., Nash, G., 2017. Development and Characterisation of a Smart Cement for CO_2 Leakage Remediation at Wellbores. Energy Procedia 114, 4147–4153. https://doi.org/10.1016/j.egypro.2017.03.1555.

Omosebi, O., Maheshwari, H., Ahmed, R., Shah, S., Osisanya, S., Hassani, S., DeBruijn, G., Cornell, W., Simon, D., 2016. Degradation of well cement in HPHT acidic environment: Effects of CO_2 concentration and pressure. Cem. Concr. Compos. 74, 54–70. https://doi.org/10.1016/j.cemconcomp.2016.09.006.

Omosebi, O.A., Sharma, M., Ahmed, R.M., Shah, S.N., Saasen, A., Osisanya, S.O., 2017. Cement Degradation in CO_2 - H_2S Environment under High Pressure-High Temperature Conditions. SPE Bergen One Day Seminar. Society of Petroleum Engineers. https://doi.org/10.2118/185932-MS.

Ouyang, X., Pan, Z., Qian, Z., Ma, Y., Ye, G., van Breugel, K., 2018. Numerical Modelling of the Effect of Filler/Matrix Interfacial Strength on the Fracture of Cementitious Composites. Materials (Basel) 11, 1362. https://doi.org/10.3390/ma11081362.

Paris, J.M., Roessler, J.G., Ferraro, C.C., DeFord, H.D., Townsend, T.G., 2016. A review of waste products utilized as supplements to Portland cement in concrete. J. Clean. Prod. 121, 1–18. https://doi.org/10.1016/j.jclepro.2016.02.013.

Postma, T.J.W., Bandilla, K.W., Celia, M.A., 2019. Estimates of CO_2 leakage along abandoned wells constrained by new data. Int. J. Greenh. Gas Control 84, 164–179. https://doi.org/10.1016/j.ijggc.2019.03.022.

Qin, L., Gao, X., 2019. Properties of coal gangue-Portland cement mixture with carbonation. https://doi.org/10.1016/j.fuel.2019.02.067. Fuel.

Raverdy, M., Brivot, F., Paillere, A.M., Dron, R., 1980. Appreciation de l'activite pouzzolanique de constituents secondaires. In: Proceedings of 7e Congrés International de La Chimie Des Ciments.

Rochelle, C.A., Czernichowski-Lauriol, I., Milodowski, A.E., 2004. The impact of chemical reactions on CO_2 storage in geological formations: a brief review. Geol. Soc. London, Spec. Publ 233, 87–106. https://doi.org/10.1144/GSL.SP.2004.233.01.07.

Saraya, M.E.-S.I., 2014. Study physico-chemical properties of blended cements containing fixed amount of silica fume, blast furnace slag, basalt and limestone, a comparative study. Constr. Build. Mater. 72, 104–112. https://doi.org/10.1016/j.conbuildmat.2014.08.071.

Schütz, M.K., Baldissera, A.F., Coteskvisk, P.M., Vecchia, F.D., Menezes, S.C., Miranda, C. R., Einloft, S., 2018. Chemical degradation of reinforced epoxy-cement composites under CO_2-rich environments. Polym. Compos. 39, E2234–E2244. https://doi.org/10.1002/pc.24589.

Schütz, M.K., dos Santos, L.M., Coteskvisk, P.M., Menezes, S.C., Einloft, S., Dalla Vecchia, F., 2019. Evaluation of CO_2 attack in wellbore class G cement: influence of epoxy resins, composites and minerals as additives. Greenh. Gases Sci. Technol. 12 https://doi.org/10.1002/ghg.1928 ghg.1928.

Sedić, K., Ukrainczyk, N., Mandić, V., Gaurina-Međimurec, N., Šipušić, J., 2020. Carbonation of Portland-Zeolite and geopolymer well-cement composites under geologic CO_2 sequestration conditions. Cem. Concr. Compos. 111, 103615 https://doi.org/10.1016/j.cemconcomp.2020.103615.

Shapakidze, E., Tsintskaladze, G., Javakhishvili, I., State, T., Kordzakhia, T., 2017. Scientific principles and practice in the use of natural mineral and industrial resources in the Georgian cement industry. Cem. Int. 16, 70–77.

SINAPI - Civil Construction Indexes. Available at: http://goo.gl/ttgltv. Accessed on Aug 18, 2020.

Snellings, R., Mertens, G., Elsen, J., 2012. Supplementary Cementitious Materials. Rev. Mineral. Geochemistry 74, 211–278. https://doi.org/10.2138/rmg.2012.74.6.

Szabó-Krausz, Z., Gál, N.E., Gável, V., Falus, G., 2020. Wellbore cement alteration during decades of abandonment and following CO_2 attack – A geochemical modelling study in the area of potential CO_2 reservoirs in the Pannonian Basin. Appl. Geochemistry 113, 104516. https://doi.org/10.1016/j.apgeochem.2019.104516.

Teodoriu, C., Bello, O., 2020. A review of cement testing apparatus and methods under CO_2 environment and their impact on well integrity prediction – Where do we stand? J. Pet. Sci. Eng. 187, 106736 https://doi.org/10.1016/j.petrol.2019.106736.

Tiong, M., Gholami, R., Rahman, M.E., 2019. Cement degradation in CO_2 storage sites: a review on potential applications of nanomaterials. J. Pet. Explor. Prod. Technol. 9, 329–340. https://doi.org/10.1007/s13202-018-0490-z.

Torsaeter, M., Opedal, N.V.D.T., Vralstad, T., Vullum, P.E., 2013. A Visual Journey Into the 3D Chemical Nanostructure of Oilwell Cement. In: SPE International Symposium on Oilfield Chemistry. Society of Petroleum Engineers, pp. 1–13. https://doi.org/10.2118/164105-MS.

Torsæter, M., Todorovic, J., Lavrov, A., 2015. Structure and debonding at cement–steel and cement–rock interfaces: Effect of geometry and materials. Constr. Build. Mater. 96, 164–171. https://doi.org/10.1016/j.conbuildmat.2015.08.005.

Tremosa, J., Mito, S., Audigane, P., Xue, Z., 2017. Experimental assessment of well integrity for CO_2 geological storage: A numerical study of the geochemical interactions between a CO_2-brine mixture and a sandstone-cement-steel sample. Appl. Geochemistry 78, 61–73. https://doi.org/10.1016/j.apgeochem.2016.12.011.

Uysal, M., Yilmaz, K., 2011. Effect of mineral admixtures on properties of self-compacting concrete. Cem. Concr. Compos. 33, 771–776. https://doi.org/10.1016/j.cemconcomp.2011.04.005.

Wakeel, S.Al, Němeček, J., Li, L., Xi, Y., Hubler, M., 2019. The effect of introducing nanoparticles on the fracture toughness of well cement paste. Int. J. Greenh. Gas Control 84, 147–153. https://doi.org/10.1016/j.ijggc.2019.03.009.

Wang, C., Chen, X., Wei, X., Wang, R., 2017. Can nanosilica sol prevent oil well cement from strength retrogression under high temperature? Constr. Build. Mater. 144, 574–585. https://doi.org/10.1016/j.conbuildmat.2017.03.221.

Yin, S., Chen, Y., Yang, Y., Huang, H., Lv, H., 2018. Effect of supplementary cementitious materials on the resistance of cement paste to carbonic acid water. Struct. Concr. 19, 1399–1408. https://doi.org/10.1002/suco.201700226.

Zha, X., Ning, J., Saafi, M., Dong, L., Dassekpo, J.B.M., Ye, J., 2019. Effect of supercritical carbonation on the strength and heavy metal retention of cement-solidified fly ash. Cem. Concr. Res. https://doi.org/10.1016/j.cemconres.2019.03.005.

Zhang, H., Ji, T., Liu, H., Su, S., 2018. Modifying recycled aggregate concrete by aggregate surface treatment using sulphoaluminate cement and basalt powder. Constr. Build. Mater. 192, 526–537. https://doi.org/10.1016/j.conbuildmat.2018.10.160.